2016

Absorbed radiation dosimetry of the D3-specific PET radioligand [18F]FluorTriopride estimated using rodent and nonhuman primate

Richard Laforest
Washington University School of Medicine in St. Louis

Morvarid Karimi
Washington University School of Medicine in St. Louis

Stephen M. Moerlein
Washington University School of Medicine in St. Louis

Jinbin Xu
Washington University School of Medicine in St. Louis

Hubert P. Flores
Washington University School of Medicine in St. Louis

See next page for additional authors

Am J Nucl Med Mol Imaging 2016;6(6):301-309
www.ajnmmi.us /ISSN:2160-8407/ajnmmi0039650

Original Article

Absorbed radiation dosimetry of the D_3-specific PET radioligand [^{18}F]FluorTriopride estimated using rodent and nonhuman primate

Richard Laforest[1], Morvarid Karimi[2†], Stephen M Moerlein[1,3], Jinbin Xu[1,3], Hubert P Flores[2], Christopher Bognar[1], Aixiao Li[1], Robert H Mach[4], Joel S Perlmutter[1,2], Zhude Tu[1]

[1]Mallinckrodt Institute of Radiology, Departments of [2]Neurology, [3]Biochemistry and Molecular Biophysics, School of Medicine, Washington University, St. Louis, MO 63110, USA; [4]Department of Radiology, Perelman School of Medicine, University of Pennsylvania, Philadelphia, PA 19104, USA. [†]Deceased.

Received September 7, 2016; Accepted November 18, 2016; Epub November 30, 2016; Published December 15, 2016

Abstract: [^{18}F]FluorTriopride ([^{18}F]FTP) is a dopamine D_3-receptor preferring radioligand with potential for investigation of neuropsychiatric disorders including Parkinson disease, dystonia and schizophrenia. Here we estimate human radiation dosimetry for [^{18}F]FTP based on the *ex-vivo* biodistribution in rodents and *in vivo* distribution in nonhuman primates. Biodistribution data were generated using male and female Sprague-Dawley rats injected with ~370 KBq of [^{18}F]FTP and euthanized at 5, 30, 60, 120, and 240 min. Organs of interest were dissected, weighed and assayed for radioactivity content. PET imaging studies were performed in two male and one female *macaque fascicularis* administered 143-190 MBq of [^{18}F]FTP and scanned whole-body in sequential sections. Organ residence times were calculated based on organ time activity curves (TAC) created from regions of Interest. OLINDA/EXM 1.1 was used to estimate human radiation dosimetry based on scaled organ residence times. In the rodent, the highest absorbed radiation dose was the upper large intestines (0.32-0.49 mGy/MBq), with an effective dose of 0.07 mSv/MBq in males and 0.1 mSv/MBq in females. For the nonhuman primate, however, the gallbladder wall was the critical organ (1.81 mGy/MBq), and the effective dose was 0.02 mSv/MBq. The species discrepancy in dosimetry estimates for [^{18}F]FTP based on rat and primate data can be attributed to the slower transit of tracer through the hepatobiliary track of the primate compared to the rat, which lacks a gallbladder. Out findings demonstrate that the nonhuman primate model is more appropriate model for estimating human absorbed radiation dosimetry when hepatobiliary excretion plays a major role in radiotracer elimination.

Keywords: [^{18}F]FluorTriopride, PET, dosimetry, Fluorine-18, D_3 receptors, Parkinson disease

Introduction

[^{18}F]FluorTriopride ([^{18}F]FTP) is a unique dopamine D_3-receptor (D3R) preferring radioligand with potential for investigation of neuropsychiatric disorders including Parkinson disease, dystonia and schizophrenia. D3R belongs to the family of D2-like receptors (D2R, D3R, D4R), which are coupled to Gi and inhibit adenyl cyclase [1, 2]. D3R like D2R are expressed in striatum, but the data suggest that D3R is expressed predominantly in ventral (limbic) and to a lesser (although still substantial) degree in dorsal (motor) striatum [3]. Various studies suggest that D2R and D3R may be regulated differently in Parkinson disease [4-6], schizophrenia [7, 8], and substance abuse [9, 10]. Recent data also hint toward abnormalities in striatal D3R in dystonia [11]. One of the major obstacles to better understanding of the D2R/D3R dynamic in such conditions has been lack of selective ligands for *in vivo* molecular imaging studies. Among numerous D2-like receptor ligands, only [^{18}F](N-methyl)benperidol (NMB) provides specificity for D2R, with a 200-fold selectivity for D2R versus D3R [11]. We have recently validated a new radioligand [^{18}F]FTP which has a 160-fold selectivity for D3R versus D2R [12]. The objective of this study is to determine the organ distribution of [^{18}F]FTP in rodent and nonhuman primate species of animals to estimate human absorbed radiation dosimetry.

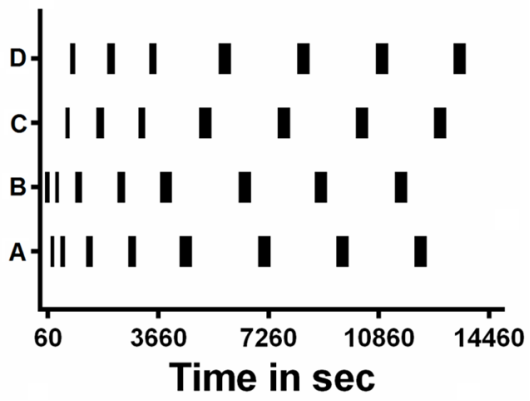

Figure 1. Schematic of data acquisition in primates using small animal PET imaging. Seven to eight successive PET scans of increasing duration were obtained in four positions: A (whole brain), B (heart and lungs), C (liver, gallbladder and kidneys), and D (urinary bladder, small and large intestines).

Specifically, we used ex-vivo biodistribution experiments in Sprague-Dawley rats and noninvasive PET imaging studies of tissue kinetics in *macaque fascicularis*. These dosimetry estimates will facilitate application of [^{18}F]FTP for PET imaging studies of D_3 receptors in human subjects.

Materials and methods

Radiopharmaceutical preparation

[^{18}F]FTP was prepared using an automated system based on published synthetic methods [12-14]. [^{18}F]Fluoride was produced by the ^{18}O(p, n)^{18}F nuclear reaction induced on an isotopically-enriched [^{18}O]water target using the Washington University RDS Eclipse cyclotron. A nucleophilic displacement reaction was used to synthesize [^{18}F]FTP starting with the corresponding mesylate and [^{18}F]fluoride. The radiolabeled product was isolated using semi-preparative HPLC. [^{18}F]FTP was reformulated in ethanolic saline for Injection, USP (1/10 v/v) and sterilized by terminal filtration. The radiochemical purity of the radiopharmaceutical product was over 95%, and the end-of-synthesis specific activity exceeded 74 TBq/mmol.

Animal protections

All applicable international, national, and institutional guidelines for the care and use of rodents and nonhuman primates were followed. Procedures used in this work were approved by the Animal Studies Committee of Washington University in Saint Louis.

Rodent biodistribution

Twenty male (200-245 gram) and 20 female (170-210 gram) Sprague Dawley rats were administered ~370 KBq of [^{18}F]FTP in 100 μL via intravenous tail vein injection. The animals were maintained in metabolic cages for collection of urine and feces excretion. Animals were euthanized in groups of four at: 5 min, 30 min, 60 min, 120 min, and 240 min post injection of [^{18}F]FTP. The organs were harvested, and the percent injected dose per gram (%ID/gram) was determined by measuring the radioactivity in weighed samples, and comparison to that of a standard sample of the injectate.

The organ residence times were calculated by numerical integration (trapezoid method) of the time activity data expressed in %ID/gram of tissue. The following initial organ activity immediately after injection was assumed based on the respective blood volumes: lungs, 5.9%; liver, 2.9%; spleen and kidneys, each 1.5%; bone, 3.7%. The remainder of activity (72%) was assigned to the blood compartment. Blood and bone mass were assumed to be 8% and 15% of the total body mass, respectively.

The cumulative activities (%ID) in the urine and feces activities were plotted as a function of time, and an uptake function [$F(t) = A_0 (1-\exp(-A_1 t))$] was fitted to the data. We then calculated a bladder residence time using the values of A_0 and A_1 in the MIRD bladder voiding model, assuming a voiding interval of 1 hr. The animal organ residence times were scaled to human organ weights according to the "relative organ mass scaling" method [15].

The above technique was employed for all organs except the small and large intestines, due to the high accumulation of radioactivity in these organs. We instead applied the percent injected dose in the entire organs as measured in the animal biodistribution experiments. The remainder of the body residence time was calculated as 70% of the injected activity deposited in blood, fat and all other unaccounted tissues. The remainder was defined as the maximum residence time of F-18 activity minus the

Table 1. Biodistribution of [^{18}F]FTP in male Sprague-Dawley rats expressed as percent injected dose per gram of tissue (%ID/g). Each set of data is the mean ± SD for n = 4 animals at each time point

	5 min	30 min	1 hour	2 hours	4 hours
Blood	0.176 ± 0.041	0.176 ± 0.012	0.146 ± 0.015	0.068 ± 0.056	0.070 ± 0.013
Lung	5.948 ± 0.354	1.601 ± 0.057	0.497 ± 0.075	0.205 ± 0.178	0.183 ± 0.023
Liver	2.999 ± 0.414	2.257 ± 0.362	1.359 ± 0.094	0.611 ± 0.515	0.707 ± 0.084
Spleen	2.693 ± 0.830	1.350 ± 0.248	0.480 ± 0.102	0.169 ± 0.147	0.165 ± 0.014
Kidney	3.725 ± 0.321	2.513 ± 0.203	1.733 ± 0.225	0.679 ± 0.550	0.770 ± 0.024
Muscle	0.176 ± 0.027	0.182 ± 0.022	0.094 ± 0.011	0.046 ± 0.038	0.048 ± 0.007
Fat	0.130 ± 0.018	0.189 ± 0.039	0.105 ± 0.021	0.043 ± 0.039	0.026 ± 0.003
Heart	1.169 ± 0.185	0.353 ± 0.025	0.195 ± 0.023	0.084 ± 0.071	0.078 ± 0.010
Brain	0.257 ± 0.023	0.171 ± 0.010	0.134 ± 0.010	0.064 ± 0.054	0.083 ± 0.011
Bone	0.564 ± 0.053	0.413 ± 0.020	0.249 ± 0.017	0.158 ± 0.132	0.292 ± 0.025
Marrow	0.836 ± 0.214	0.689 ± 0.042	0.412 ± 0.038	0.143 ± 0.127	0.084 ± 0.034
Testes/Uterus	0.152 ± 0.014	0.223 ± 0.010	0.202 ± 0.011	0.119 ± 0.101	0.119 ± 0.017
Prostate/Ovaries	0.587 ± 0.247	0.734 ± 0.086	0.736 ± 0.310	0.340 ± 0.326	0.088 ± 0.084
Adrenals	3.767 ± 1.049	5.838 ± 0.698	3.868 ± 1.002	1.806 ± 1.551	0.798 ± 0.345
Thyroid	0.863 ± 0.158	0.305 ± 0.209	0.238 ± 0.004	0.097 ± 0.078	0.127 ± 0.031
Pancreas	1.893 ± 0.208	1.094 ± 0.062	0.398 ± 0.067	0.121 ± 0.106	0.095 ± 0.016
Thymus	0.838 ± 0.081	0.695 ± 0.052	0.511 ± 0.057	0.225 ± 0.185	0.158 ± 0.030
Stomach	0.372 ± 0.129	0.410 ± 0.085	0.344 ± 0.079	0.170 ± 0.163	0.057 ± 0.017
Small intestine	3.239 ± 0.500	4.986 ± 0.959	3.283 ± 1.191	0.848 ± 0.730	0.392 ± 0.038
Upper large intestine	0.703 ± 0.067	2.718 ± 0.972	9.278 ± 1.151	7.996 ± 6.584	1.645 ± 0.565
Lower large intestine	0.234 ± 0.007	0.202 ± 0.013	0.255 ± 0.048	0.356 ± 0.356	6.296 ± 1.053

Table 2. Biodistribution of [^{18}F]FTP in female Sprague-Dawley rats expressed as percent injected dose per gram of tissue (%ID/g). Each set of data is the mean ± SD for n = 4 animals at each time point

	5 min	30 min	1 hour	2 hours	4 hours
Blood	0.176 ± 0.041	0.176 ± 0.012	0.146 ± 0.015	0.068 ± 0.056	0.070 ± 0.013
Lung	5.948 ± 0.354	1.601 ± 0.057	0.497 ± 0.075	0.205 ± 0.178	0.183 ± 0.023
Liver	2.999 ± 0.414	2.257 ± 0.362	1.359 ± 0.094	0.611 ± 0.515	0.707 ± 0.084
Spleen	2.693 ± 0.830	1.350 ± 0.248	0.480 ± 0.102	0.169 ± 0.147	0.165 ± 0.014
Kidney	3.725 ± 0.321	2.513 ± 0.203	1.733 ± 0.225	0.679 ± 0.550	0.770 ± 0.024
Muscle	0.176 ± 0.027	0.182 ± 0.022	0.094 ± 0.011	0.046 ± 0.038	0.048 ± 0.007
Fat	0.130 ± 0.018	0.189 ± 0.039	0.105 ± 0.021	0.043 ± 0.039	0.026 ± 0.003
Heart	1.169 ± 0.185	0.353 ± 0.025	0.195 ± 0.023	0.084 ± 0.071	0.078 ± 0.010
Brain	0.257 ± 0.023	0.171 ± 0.010	0.134 ± 0.010	0.064 ± 0.054	0.083 ± 0.011
Bone	0.564 ± 0.053	0.413 ± 0.020	0.249 ± 0.017	0.158 ± 0.132	0.292 ± 0.025
Marrow	0.836 ± 0.214	0.689 ± 0.042	0.412 ± 0.038	0.143 ± 0.127	0.084 ± 0.034
Testes/Uterus	0.152 ± 0.014	0.223 ± 0.010	0.202 ± 0.011	0.119 ± 0.101	0.119 ± 0.017
Prostate/Ovaries	0.587 ± 0.247	0.734 ± 0.086	0.736 ± 0.310	0.340 ± 0.326	0.088 ± 0.084
Adrenals	3.767 ± 1.049	5.838 ± 0.698	3.868 ± 1.002	1.806 ± 1.551	0.798 ± 0.345
Thyroid	0.863 ± 0.158	0.305 ± 0.209	0.238 ± 0.004	0.097 ± 0.078	0.127 ± 0.031
Pancreas	1.893 ± 0.208	1.094 ± 0.062	0.398 ± 0.067	0.121 ± 0.106	0.095 ± 0.016
Thymus	0.838 ± 0.081	0.695 ± 0.052	0.511 ± 0.057	0.225 ± 0.185	0.158 ± 0.030
Stomach	0.372 ± 0.129	0.410 ± 0.085	0.344 ± 0.079	0.170 ± 0.163	0.057 ± 0.017
Small intestine	3.239 ± 0.500	4.986 ± 0.959	3.283 ± 1.191	0.848 ± 0.730	0.392 ± 0.038
Upper large intestine	0.703 ± 0.067	2.718 ± 0.972	9.278 ± 1.151	7.996 ± 6.584	1.645 ± 0.565
Lower large intestine	0.234 ± 0.007	0.202 ± 0.013	0.255 ± 0.048	0.356 ± 0.356	6.296 ± 1.053

Table 3. Organ residence times of [^{18}F]FTP scaled to human males and females based on male and female rat biodistribution data

Organ	Residence Time Males-(min)	Residence Time Females-(min)
Blood	5.2 ± 1.2	3.9 ± 0.5
Lung	8.2 ± 0.8	8.5 ± 1.9
Liver	18.8 ± 3.9	20.1 ± 3.5
Spleen	0.91 ± 0.24	1.15 ± 0.23
Kidney	3.4 ± 0.6	3.16 ± 0.49
Muscle	18.6 ± 4.3	11.0 ± 2.7
Fat	4.4 ± 1.3	3.19 ± 1.3
Heart	0.58 ± 0.11	0.56 ± 0.11
Brain	1.26 ± 0.25	1.05 ± 0.16
Bone	24.2 ± 4.5	18.57 ± 3.2
Marrow	2.73 ± 0.66	4.77 ± 1.1
Testes	0.05 ± 0.01	
Prostate	0.064 ± 0.03	
Adrenals	0.33 ± 0.11	0.233 ± 0.07
Thyroid	0.037 ± 0.012	0.039 ± 0.008
Pancreas	0.34 ± 0.05	0.35 ± 0.04
Thymus	0.061 ± 0.013	0.081 ± 0.01
Stomach	0.27 ± 0.106	0.54 ± 0.16
Small intestines	13.1 ± 5.6	14.0 ± 5.6
Upper large intestines	48.3 ± 25.2	68.8 ± 7.5
Lower large intestines	32.8 ± 3.1	38.6 ± 4.5
Uterus		0.21 ± 0.04
Ovaries		0.09 ± 0.02
Excreted	20	15
Remainder of the body	3.9	3.0

sum of observed residence times in specific organs minus the excreted residence time.

The scaled human residence times from these rodent experiments were entered in the program OLINDA/EXM 1.1 for F-18 in the adult human male and female anthropomorphic models [16].

Nonhuman primate tissue distribution

Two male and a female *macaque fascicularis* underwent whole-body scanning for approximately 3 hrs using a Siemens MicroPET-F220. The animals weighed 7.2 (male 1), 6.4 (male 2) and 4.5 (female) kg, and received 167, 176 and 143 MBq of [^{18}F]FTP respectively. The first animal (male 1) was scanned twice, and received 190 MBq of [^{18}F]FTP for the second scan. The animals were prepared for imaging as previously described [17, 18].

Data acquisition

Prior to radioligand injection, we collected four 30 min transmission scans to cover four body sections: A (whole brain), B (heart and lungs), C (liver, gallbladder and kidneys), and D (urinary bladder, small and large intestines). Starting immediately after i.v. injection of [^{18}F]FTP, seven to eight sequential PET scans were performed for each of the four sections (**Figure 1**). No loss of urine or fecal matter was observed in the animals during the scans. For one of the animals (male 1), arterial blood samples were obtained during a total scanning session of approximately 4 hrs. Most of the blood samples were taken in the first 3 min to ensure adequate description of the total radioactivity within the arterial blood compartment, Afterwards, longer sampling times were used over the 4 hrs study. The radioactivity content in each blood sample was measured in a well counter that was cross-calibrated with the PET scanner.

PET image analysis

The reconstructed image resolution at the center of the field of view for the PET studies was < 2.0 mm full width half maximum (FWHM) for all 3 dimensions. PET image counts were calibrated to a dose calibrator to facilitate comparison of PET measurements to MBq of F-18. For some organs (whole brain, heart, lungs, urinary bladder), regions of interest (ROIs) were drawn to entirely encompass the organ using ASIPro VM™ MicroPET analysis software (Siemens PreClinical Solutions, Knoxville, TN). For others (liver, kidney, and gallbladder), we could not delineate an appropriate ROI. Hence, we chose several small representative ROIs that contained the highest observed radioactivity concentrations within the specific organ. The average radioactivity concentrations of these representative ROIs were multiplied by the entire organ weight to give a liberal estimate of the radioactivity within the total organ. This approach will lead to slight overestimation of the organ values, but the error in the estimate tends toward increased subject safety.

The calculated activity in the whole organ was plotted as a function of time to yield the organ

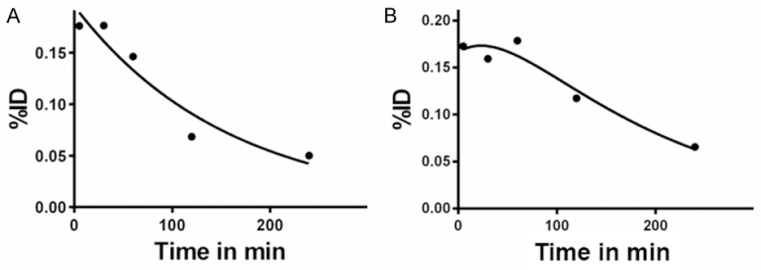

Figure 2. Blood time-activity curves for [^{18}F]FTP expressed in percentage of injected dose (%ID) per organ in male (A) and female (B) rats (n = 4 at each time point).

Table 4. Estimated human absorbed radiation dose for [^{18}F]FTP (mSv/MBq) from rodent biodistribution data

Organ	Dose (mSv/MBq)	
	Males	Females
Adrenals	0.06	0.06
Brain	0.01	0.01
Breasts	0.01	0.01
Gallbladder wall	0.03	0.04
Lower large intestine wall	*0.34*	*0.43*
Small Intestines wall	0.08	0.11
Stomach Wall	0.02	0.02
Upper large intestine wall	*0.33*	*0.48*
Heart muscle	0.01	0.02
Kidneys	0.05	0.05
Liver	0.05	0.06
Lungs	0.03	0.04
Muscle	0.01	0.01
Ovaries	0.00	0.09
Pancreas	0.02	0.03
Red Marrow	0.02	0.03
Bones (osteogenic cells)	0.04	0.04
Skin	0.01	0.01
Spleen	0.02	0.01
Testes	0.01	0.00
Thymus	0.01	0.02
Thyroid	0.01	0.01
Urinary bladder wall	0.05	0.05
Uterus	0.02	0.04
Total Body	0.01	0.02

Table 5. Estimated effective dose and effective dose equivalent for [^{18}F]FTP in human adult males and females based on the rodent biodistribution data

	Males	Females
Effective Dose (mSv/MBq)	0.07	0.1
Effective Dose Equivalent (mSv/MBq)	0.064	0.1

time-activity curves. Organ residence times were computed from the analytical integration of the multi-exponential fitted onto the decay-corrected time-activity curves using GraphPad Prism6 software. The maximum theoretical residence time ($T_{1/2}$/ln(2) = 2.64 hrs for F-18) minus the sum of measured residence times was assigned to the remainder of the body as unspecific activity. The urinary bladder time activity curve was also fitted with an uptake function to provide the MIRD bladder model parameters needed to calculate the bladder activity residence time. For this estimation, 2 hrs bladder voiding intervals were used.

The blood time-activity curve for nonhuman primate data was integrated using the trapezoidal rule to yield the blood residence time. The blood activity in units of MBq/mL was converted to percent injected dose assuming a blood volume of 8% of body weight and the injected dose (175.5 MBq). Finally, 5% of the blood volume was assumed to be present in the left ventricle at all times.

The calculated residence times (T) were scaled from animal to human based on the equation:

$$T_{human} = T_{animal}\left(\frac{M_{human}^{organ}}{M_{human}^{body}}\right)\left(\frac{M_{animal}^{body}}{M_{animal}^{organ}}\right) \quad (1)$$

Where T is the residence time and M is the mass (organ or total body).

We used human male and female organ weights in OLINDA/EXM [19] for the adult male and adult female models. The percentage body weight was applied for the kidney, liver, and heart as reported previously for male and female macaque fascicularis [20]. We used the gallbladder and bladder percentages of total body weight as determined *ex vivo* in the past, and the organ weights for the brain and lungs were based on their measured volume and an assumed density of 1.0 g/cm^3.

The scaled human residence times were entered in the program OLINDA/EXM 1.1 for F-18 following the adult human male and female anthropomorphic models, with the assumption that 10% of the blood residence time is in the heart and bone activity is equal

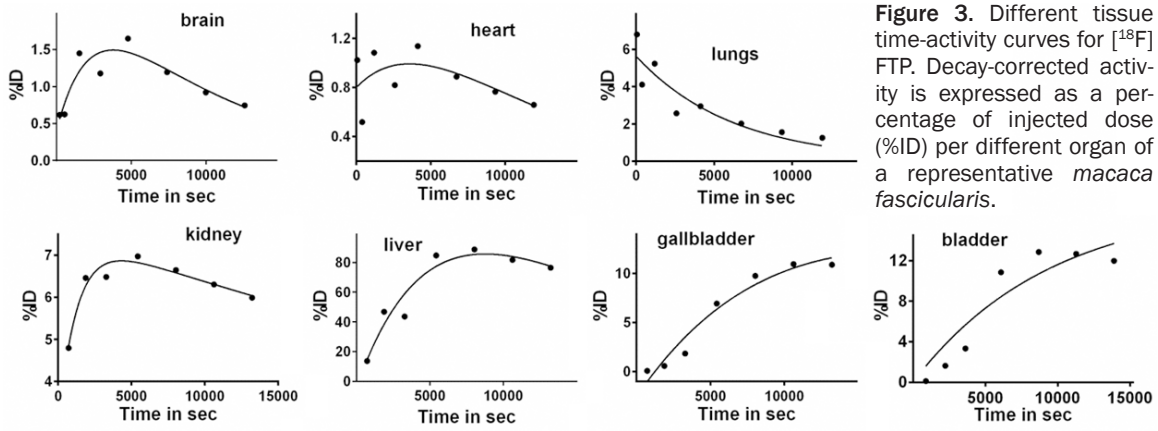

Figure 3. Different tissue time-activity curves for [^{18}F]FTP. Decay-corrected activity is expressed as a percentage of injected dose (%ID) per different organ of a representative *macaca fascicularis*.

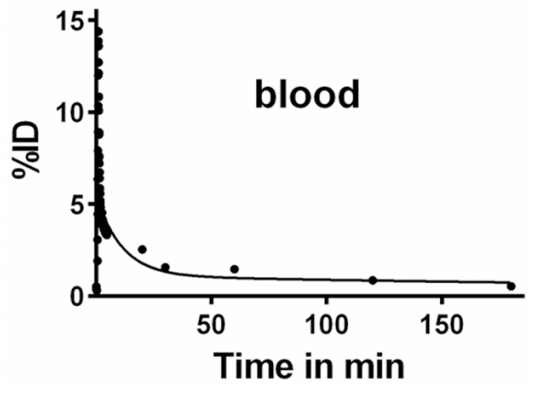

Figure 4. Blood time-activity curve based on arterial blood sampling in a male *macaca fascicularis* following the intravenous injection of [^{18}F]FTP.

part cortical and trabecular. The content within the intestines was used as the source of absorbed radiation to the intestines.

Results

Rodent biodistribution

The male and female rat biodistribution data are presented in **Tables 1** and **2**, respectively. The data is very similar for the two species. Both show predominant accumulation of radioactivity in the small intestines which peaks at 30 minutes, followed by accumulation in the upper large intestine that is maximum at about 1 hr. There was relatively modest localization of activity in liver and kidney.

Residence times and dosimetry from rodent biodistribution data

Organ residence times scaled to human organ weights are presented in **Table 3**. In The largest residence times were observed in the small and large intestines. Otherwise, the internal organ with the largest accumulation was the liver. The residence time in the blood was low at approximately 0.17 min and was characterized by a single exponential clearance with a biological half-life of 173 min for both male and female groups (n = 4 at each time point) (**Figure 2**).

For the male group, the fit on urine data provided A_0 = 22%ID and A_1 = 0.90 hr^{-1} with a bladder residence time of 4.6 min and an excreted residence time of 20.0 min. The fit on the feces data provided A_0 = 0.07%ID and A_1 = 0.5 hr^{-1} with an excreted residence time of 0.063 min. Combined data for urine and feces resulted in an excreted residence time of 20 min. For the female group, the fit of the urine data provided A_0 =15%ID and A_1 = 1.12 hr^{-1} with a bladder residence time of 2.85 min and an excreted residence time of 14.9 min. The fit of the feces data provided A_0 = 0.04%ID and A_1 = 0.75 hr^{-1} with an excreted residence time of 0.042 min. Combined data for urine and feces resulted in an overall excreted residence time of 15 min.

Estimates of human organ absorbed radiation doses for the adult human male and female are presented in **Tables 4** and **5**, respectively. The uncertainty of the dose estimates is proportional to the uncertainties in the respective organ residence times.

Nonhuman primate biodistribution

The representative sagittal image of [^{18}F]FTP indicates the *macaque fascicularis* has relative high gallbladder uptake within 10 min data collection at 190 min post injection shown in Figure S1A and representative transverse

Table 6. Organ residence times (hr) for [^{18}F]FTP in based on PET image data from *macaque fascicularis*

Organ	Residence Time (hr)		
	#1 (male)	#2 (male)	#3 (female)
Liver	1.85	1.27	1.83
Heart	0.02	0.09	0.02
Rain	0.04	0.05	0.07
Lungs	0.05	0.07	0.01
Gallbladder	0.15	0.02	0.38
Kidneys	0.13	0.19	0.11
Urinary bladder	0.13	0.06	0.21
Blood assigned to the left ventricle cavity	0.002	0.002	0.002
Remainder of the body	0.26	0.87	0.01

Table 7. Effective dose and effective dose equivalent for [^{18}F]FTP in human adult males and females estimated from *in vivo* distribution data in *macaque fascicularis*

	Males	Females
Effective Dose (mSv/MBq)	0.26	0.37
Effective Dose Equivalent (mSv/MBq)	0.24	0.37

image of [^{18}F]FTP indicates animal has high lung uptake with 2 min data collection beginning 6 min post injection Figure S1B.

Figure 3 shows the time activity curves compiled from sequential imaging of a male *macaca fascicularis*. The time activity data were fitted with a function composed of single or combined exponentials. Least square minimization was performed to find the best fitting parameters.

Residence times and dosimetry estimation

The time-activity data for blood was collected for the second male *macaca fascicularis* only, and is shown in **Figure 4**. We calculated a heart chamber residence time of 0.091 min based on the blood residence time of 1.82 min, a value that was employed for all the animals. The calculated residence times are reported in **Table 6**.

Human adult male and female absorbed radiation dosimetry was estimated from data derived from residence times for the animals and the OLINDA/EXM model. These data are presented in **Table 7**.

Discussion

Rat *ex vivo* biodistribution data showed that [^{18}F]FTP was retained predominantly in the intestines, suggesting relatively rapid clearance of the radioactivity from the liver into the small intestines and subsequent transfer to the large intestines. The organ having the largest absorbed radiation dose was the wall of the large intestines for both male and females, making the intestines the dose limiting organ (0.32-0.49 mGy/MBq). As an estimate of human dosimetry, the Effective Dose (ED) was 0.07 mSv/MBq in male and 0.1 mSv/MBq in female. Although the rodent data indicates a maximum injected dose of 480 MBq to correspond to an effective dose (ED) below 50 mSv, the radiation dose to the intestes is the dose limiting factor. Indeed, the rat model projects an injected dose of 111 MBq will result in a radiation dose of approximately 50 mGy to the intestinal wall, with less than 30 mGy delivered to the gonads, red marrow or whole body.

By contrast, data from the imaging studies of nonhuman primate demonstrated high retention of the radiotracer in the liver and gallbladder, indicating predominant hepatobiliary clearance. The image data from the *macaque* studies demonstrate a much longer residence time in the liver, and the absence of activity in the intestines. These findings reflect the much slower transfer of [^{18}F]FTP and/or its radioactive metabolites through the hepatobiliary track in primates compared to rodents. As a result of this difference in tracer disposition, the critical organ based on the *macaque* data was the gallbladder wall (estimated human dose 2.78 mGy/MBq) and a lower Effective Dose (0.02 mSv/MBq) compared to estimates based on rodent data. An injected dose of 181 MBq of [^{18}F]FTP will yield a an estimated human absorbed radiation dose of approximately 50 mGy to the gallbladder, and less than 30 mGy to the gonads, red marrow or whole body.

Conclusions

The human absorbed radiation dosimetry of new radiopharmaceutical can be estimated in preclinical studies of radiotracer disposition in

rodent and nonhuman primate. In these measurements, it is important to be aware of species differences when estimating human dosimetry. As this study of the D_3 radioligand [^{18}F]FTP shows, dramatic differences can arise in human dose estimates based on rodent and nonhuman primate models. The discrepancy between the critical organs estimated using rodent and nonhuman primate data most likely reflects the lack of a gallbladder in rodents. This crucial observation is a caveat against estimation of human dosimetry from rodent data for radiopharmaceuticals with hepatobiliary clearance.

Acknowledgements

This work was supported by NIH grants NS058714, NS41509, NS075321, NS075527, and MH092797; American Parkinson Disease Association (APDA) Center for Advanced PD Research at Washington University; Greater St. Louis Chapter of the APDA; McDonnell Center for Higher Brain Function; Barnes-Jewish Hospital Foundation (Elliot Stein Family Fund for PD Research & the Parkinson disease Research Fund) and by the Department of Radiology of Washington University. We like to thank the staff members of the Small Animal PET/CT Imaging Facility of Washington University Medical School for the rodent dissection experiments. We like also to thank the staff member of the Cyclotron Facility for production of the F-18 tracer.

Disclosure of conflict of interest

None.

Address correspondence to: Dr. Zhude Tu, Mallinckrodt Institute of Radiology, School of Medicine, Washington University, 510 South Kingshighway Boulevard, St. Louis, MO 63110, USA. Tel: 314-362-8487; Fax: 314-362-8555; E-mail: tuz@mir.wustl.edu

References

[1] Civelli O, Bunzow JR and Grandy DK. Molecular diversity of the dopamine receptors. Annu Rev Pharmacol Toxicol 1993; 32: 281-307.

[2] Griffon N, Pilon C, Sautel F, Schwartz JC and Sokoloff P. Two intracellular signaling pathways for the dopamine D3 receptor: opposite and synergistic interactions with cyclic AMP. J Neurochem 1997; 68: 1-9.

[3] Sun J, Xu J, Cairns NJ, Perlmutter JS and Mach RH. Dopamine D1, D2, D3 receptors, vesicular monoamine transporter type-2 (VMAT2) and dopamine transporter (DAT) densities in aged human brain. PLoS One 2012; 7: e49483.

[4] Ryoo HL, Pierrotti D and Joyce JN. Dopamine D3 receptor is decreased and D2 receptor is elevated in the striatum of Parkinson's disease. Mov Disord 1998; 13: 788-797.

[5] Levesque D, Martres MP, Diaz J, Griffon N, Lammers CH, Sokoloff P and Schwartz JC. A paradoxical regulation of the dopamine D3 receptor expression suggests the involvement of an anterograde factor from dopamine neurons. Proc Natl Acad Sci U S A 1995; 92: 1719-1723.

[6] Morissette M, Goulet M, Grondin R, Blanchet P, Bedard PJ, Di PT and Levesque D. Associative and limbic regions of monkey striatum express high levels of dopamine D3 receptors: effects of MPTP and dopamine agonist replacement therapies. Eur J Neurosci 1998; 10: 2565-2573.

[7] Gurevich EV, Bordelon Y, Shapiro RM, Arnold SE, Gur RE and Joyce JN. Mesolimbic dopamine D3 receptors and use of antipsychotics in patients with schizophrenia. A postmortem study. Arch Gen Psychiatry 1997; 54: 225-232.

[8] Zhang L, Yokoi F, Parsons DS, Standaert DG and Li Y. Alteration of striatal dopaminergic neurotransmission in a mouse model of DYT11 myoclonus-dystonia. PLoS One 2012; 7: e33669.

[9] Volkow ND, Tomasi D, Wang GJ, Logan J, Alexoff DL, Jayne M, Fowler JS, Wong C, Yin P and Du C. Stimulant-induced dopamine increases are markedly blunted in active cocaine abusers. Mol Psychiatry 2014; 19: 1037-1043.

[10] Staley JK and Mash DC. Adaptive increase in D3 dopamine receptors in the brain reward circuits of human cocaine fatalities. J Neurosci 1996; 16: 6100-6106.

[11] Karimi M, Moerlein SM, Videen TO, Luedtke RR, Taylor M, Mach RH and Perlmutter JS. Decreased Striatal Dopamine Receptor Binding in Primary Focal Dystonia: A D2 or D3 Defect? Mov Disord 2011; 26: 100-106.

[12] Tu Z, Li S, Cui J, Xu J, Taylor M, Ho D, Luedtke RR and Mach RH. Synthesis and pharmacological evaluation of fluorine-containing D(3) dopamine receptor ligands. J Med Chem 2011; 54: 1555-1564.

[13] Mach RH, Tu Z, Xu J, Li S, Jones LA, Taylor M, Luedtke RR, Derdeyn CP, Perlmutter JS and Mintun MA. Endogenous dopamine (DA) competes with the binding of a radiolabeled D_3 receptor partial agonist in vivo: A positron emission tomography study. Synapse 2011; 65: 724-732.

[14] Tu Z, Li S, Xu J, Chu W, Jones LA, Luedtke RR and Mach RH. Effect of cyclosporin A on the uptake of D_3-selective PET radiotracers in rat brain. Nucl Med Biol 2011; 38: 725-739.
[15] Stabin MG and Siegel JA. Physical models and dose factors for use in internal dose assessment. Health Phys 2003; 85: 294-310.
[16] Lee C, Lodwick D and Bolch WE. NURBS-based 3-D anthropomorphic computational phantoms for radiation dosimetry applications. Radiat Prot Dosimetry 2007; 127: 227-232.
[17] Antenor-Dorsey JA, Laforest R, Moerlein SM, Videen TO and Perlmutter JS. Radiation dosimetry of N-([11C]methyl)benperidol as determined by whole-body PET imaging of primates. Eur J Nucl Med Mol Imaging 2008; 35: 771-778.
[18] Karimi M, Tu Z, Yue X, Zhang X, Jin H, Perlmutter JS and Laforest R. Radiation dosimetry of [(18)F]VAT in nonhuman primates. EJNMMI Res 2015; 5: 73.
[19] Stabin MG, Sparks RB and Crowe E. OLINDA/EXM: the second-generation personal computer software for internal dose assessment in nuclear medicine. J Nucl Med 2005; 46: 1023-1027.
[20] Drevon-Gaillot E, Perron-Lepage MF, Clement C and Burnett R. A review of background findings in cynomolgus monkeys (Macaca fascicularis) from three different geographical origins. Exp Toxicol Pathol 2006; 58: 77-88.

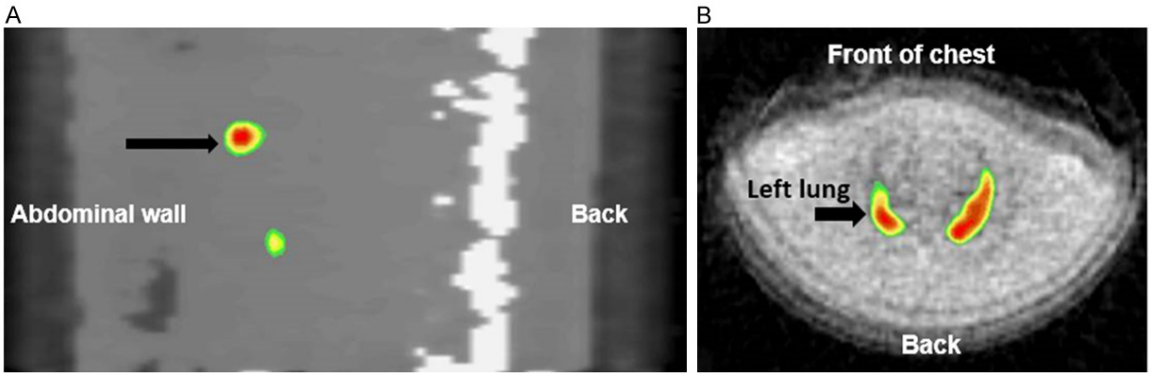

Figure S1. A. Representative Sagittal PET Image of [^{18}F]FTP in the abdomen of monkey. Sagittal view through abdomen with left of image toward the abdominal wall and right of the image to the back. This is a PET image with 10 min data collection beginning with 190 min post [^{18}F]FTP administration. The arrow indicates uptake of [^{18}F]FTP in the gallbladder. The lower warm spot is in the bowel. Warmer colors indicate higher uptake. The image is scaled to the slice maximum. The bony spine shows as white on the right of the attenuation image. B. Representative transverse PET Image of [^{18}F]FTP in the abdomen of monkey. Transverse view through chest with top of the image toward the abdominal wall and bottom of the image to the back. This is a PET image with 2 min data collection beginning 6 min after [^{18}F]FTP administration. The arrow indicates the left lung. The animal is lying supine in the scanner which increases the blood flow toward the back (due to gravity). The lungs have high uptake of [^{18}F]FTP in this early scan. Warmer colors indicate higher uptake. The image is scaled to the slice maximum.